

A Hybrid 3d Reconstruction / Registration Algorithm for Correction of Head Motion in Emission Tomography.

B.F. Hutton¹, A. Kyme², Y.H. Lau¹, D.W. Skerrett¹, R.R. Fulton³.

¹Departments of Medical Physics and Nuclear Medicine & Ultrasound, Westmead Hospital, Sydney.

²Department of Physics, University of NSW, Sydney.

³Department of PET & Nuclear Medicine, Royal Prince Alfred Hospital, Sydney.

Abstract

Even with head restraint small head movements can occur during data acquisition for emission tomography, sufficiently large to result in detectable artifacts in the final reconstruction. Direct measurement of motion can be cumbersome and difficult to implement, whereas previous attempts to correct for motion based on measured projections have been limited to simple translation orthogonal to the projection. A fully 3d algorithm is proposed that estimates the patient orientation at any time based on the projection of motion-corrupted data, with incorporation of the measured motion within subsequent OSEM sub-iterations. Preliminary studies have been performed using a digital version of the Hoffman brain phantom. Movement was simulated by constructing a mixed set of projections in two discrete positions of the phantom. The algorithm determined the phantom orientation that best aligned each constructed projection with its corresponding measured projection. In the case of simulated movement of 24 of 64 projections, all mis-positioned projections were correctly identified. The algorithm resulted in a reduction of mean square difference (MSD) between motion corrected and motion-free reconstructions compared to the MSD between uncorrected and motion-free reconstructions by a factor of 2.7.

I. INTRODUCTION

In both single photon emission computed tomography (SPECT) and positron emission tomography (PET) data acquisition occurs over a relatively long time, typically in the range of 1-30 minutes. Consequently patient motion is quite common. Since the fundamental reconstruction algorithms operate on the assumption that the object to be imaged is stationary during acquisition, any movement results in potential artifacts in the reconstruction. In the case of brain studies, head restraints are normally used, however, particularly with non-compliant patients, movement can still occur. Even with the small movements recorded with head restraint, measurable effects can be demonstrated [1].

Several groups have used direct measurement to detect or estimate motion with subsequent correction. These include use of radio-frequency devices [2], video monitoring [3], optical trackers [4] or less expensive mechanical devices [5]. Correction in PET has included direct modification of individual coincidence lines of response [2] or acquisition of a new frame when significant motion is detected [3], [6]. In

SPECT (or in non-ring PET systems) there is further complication since motion may occur during detector rotation so that there may be incomplete data corresponding to a stationary position of the patient. A method of direct 3d reconstruction incorporating the average location for each projection has been developed previously by our group [7]. Others have also suggested alternative approaches to 3d reconstruction incorporating motion information [e.g. 8]. In general, measurement devices can be cumbersome or expensive and usually require careful calibration. Attempts to correct for motion without direct measurement have been limited to the translation of projections only [9], [10], or registration of multiple frames [11]. Neither of these techniques provides a general solution for data-driven motion correction. The purpose of this paper is to present a hybrid technique that involves registration to determine the 3d orientation of the patient at each projection angle, incorporating this information in a fully 3d reconstruction.

II. METHODS

A. Description of the Algorithm

For convenience the method will be described for the geometry typical of multi-detector SPECT systems, however, the approach is applicable generally to a wide range of detector or collimator geometry, whether PET or SPECT. A dual right-angled SPECT system is illustrated in Fig. 1(a). Reconstruction is normally performed using the measured projections to reconstruct individual planes. If motion of the object has occurred during data acquisition some projections will be incorrectly located relative to the object during conventional multi-plane 2d reconstruction. However, provided movement is relatively small, the multi-plane reconstruction will provide a reasonable estimate of the object activity distribution. This corrupted estimate can be used to construct 2d projections, which can be directly compared with the measured projections.

The assumption made is that the errors introduced by the corrupted reconstruction estimate are outweighed by errors due to misplaced projections. We determine the 3d orientation of the object that will result in the optimal match between constructed and measured projections. This is achieved by implementing a fully 3d registration of the object where we optimize 6 parameters for object position and orientation using the simplex algorithm (see Fig. 1(b)). The cost function is formulated as the sum of squared differences between the constructed (forward-projected) and

measured 2d projections, where the orientation of the object determines the direction of the constructed projection. Note that the cost function is evaluated for all projections acquired at the same time (i.e. the right-angled pair of projections in our case).

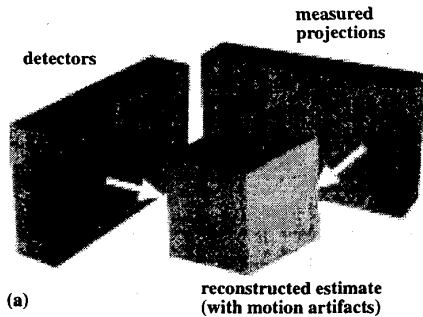


Fig. 1(a): For a dual-detector SPECT system the measured projections are used to reconstruct an estimate of the activity distribution in the object. This reconstructed estimate may contain motion artifacts.

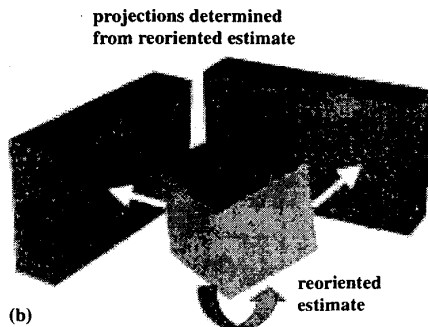


Fig. 1(b): The reconstructed estimate is reoriented so as to provide the best match between constructed projections and the original measured projections.

Once the optimal location is determined, the projections will be correctly located so that they can be used to update the solution or contribute to a correctly constructed 3d reconstruction. We utilize a useful property of the ordered subsets expectation maximization (OSEM) algorithm [12]. Since each sub-iteration involves use of only a subset of projections, these can be chosen so as to include projections recorded when the object was stationary. A similar approach was used previously for incorporation of measured motion in 3d reconstruction [7]. In the case of a dual-detector system, the subset contains the pair of projections for which the object orientation has been optimized. The process is repeated for each projection pair, progressively improving the reconstructed estimate with correctly aligned projections.

B. Demonstration of feasibility

In order to assess the operation of the algorithm a digital version of the Hoffman brain phantom was used. Complete projection sets ($64 \times 64 \times 64$) were constructed for various different orientations of the phantom, one of which was used

as a motion-free reference. Projections included attenuation and distance-dependent resolution, but no scatter. Combining projections selected from both data sets then created a simulated motion. To demonstrate feasibility simple one-dimensional reorientations were examined (translation in x direction or rotation around x axis). The following tests were performed for each orientation.

- How well are incorrect projections identified?* The motion free reconstruction was used to generate projections, which were compared with both the motion-free projections and the reoriented projections. The sum of square differences (SSD) between generated and 'measured' projections was averaged over all angles.
- How does motion influence the reconstruction?* Motion corrupted data sets were constructed with either 4 or 12 orthogonal pairs of reoriented projections from the total of 64. The degree of distortion in the reconstruction was assessed using the mean square difference (MSD) between motion-corrupted and motion-free reconstructions.
- Can projection orientation still be recognised using the corrupt reconstruction?* Using the corrupt reconstruction, projections were generated and compared against motion-free versus reoriented projections. The ratio of mean SSD for the reoriented versus motion-free projections was calculated.
- Can the correct orientation of projections be found?* For each simulated orientation of the phantom, the corrupted reconstruction was reoriented incrementally and the SSD between constructed and measured projections calculated.

C. Investigating the limits of applicability

Each of the six rotation and translation parameters were individually investigated to better understand the behaviour of the projector in determining correct projection position. As in the previous experiment change of position was simulated for a number of projections (12/64) and the resulting 'corrupted' reconstruction was reoriented by varying degrees prior to constructing projections. The MSD between constructed and original projections for either motion-free or repositioned projections, was measured for each object orientation. Results are provided for noise-free data and for (x1, x2) noise representative of clinical brain SPECT (~50k counts per projection).

D. Preliminary validation

As a preliminary validation of the complete motion correction algorithm the same Hoffman brain phantom was used. In this case the single reorientation applied was (2mm, -1mm, 2mm, 4deg, -2deg, 4deg) for translation and rotation in 3d. Twelve projection pairs were selected from the reoriented data set and substituted in the original motion-free set of projections. The motion-free data were reconstructed using OSEM with subset size 2 (1 iteration) as

a reference. The motion-corrupted data were also reconstructed and the mean squared difference (MSD) between motion-free and uncorrected reconstructions evaluated (MSD-corrup). The motion-corrupted data also were reconstructed using the proposed motion correction algorithm as follows:

- a. Using the motion-corrupted reconstruction as a starting estimate, projections were constructed by forward projection, including attenuation. The sum of squared differences (SSD) between each pair of constructed and measured projections was calculated and used to identify projections that were mis-positioned.
- b. For the most mis-positioned pair of projections the orientation of the current reconstruction estimate was adjusted so as to minimize the SSD between the constructed and measured projections. The reconstruction was updated by a single sub-iteration OSEM using the reoriented estimate and corresponding projections.
- c. The updated reconstruction estimate can be used to determine the best object orientation for the next pair of projections. In our case, the update was used to confirm that the current orientation was sufficient for the next projection.
- d. The final motion corrected reconstruction was compared with the motion free reconstruction by calculating the MSD between motion-free and motion-corrected reconstructions (MSD-corrected).

III. RESULTS

A. Demonstration of feasibility

Table 1
How well are incorrect projections identified?

	SSD/10 ³	SSD/ SSD (no motion)
No motion	0.60	
1° (x axis)	0.91	1.51
2° (x axis)	1.43	2.38
4° (x axis)	3.68	6.13
0.5 pixels	2.26	3.77
1.0 pixels	5.79	9.65
2.0 pixels	18.98	31.63

Table 2
How does motion influence the reconstruction?

	MSD: moved for 8/64 projections	MSD: moved for 24/64/projections
1° (x axis)	5.6	16.7
2° (x axis)	8.1	26.4
4° (x axis)	16.4	61.1
0.5 pixels	16.7	52.6
1.0 pixels	44.6	147.0
2.0 pixels	129.0	478.0

The results of the feasibility study are summarised in Tables 1-4. Even for small reorientation (1 degree or 0.5 pixels) there is a measurable difference between the SSD for reoriented versus motion-free projections (Table 1). As expected the differences increase as the magnitude of reorientation increases. The degree of distortion in the reconstruction due to incorrectly positioned projections also increases with increasing magnitude of reorientation and is quite sizeable for large translations (Table 2).

Table 3
Can projection orientation still be recognised using the corrupt reconstruction?

	SSD ratio 8/64 projections	SSD ratio 24/64/projections
1° (x axis)	1.68	2.65
2° (x axis)	2.57	3.24
4° (x axis)	4.28	4.27
0.5 pixels	3.81	5.48
1.0 pixels	8.40	9.80
2.0 pixels	20.20	16.49

Table 4
Can the correct orientation of projections be found (rotation in x axis)?

Constructed projections		Original position of projections			
		No motion	1°	2°	4°
No motion	8/64	0.6			
	24/64	0.6			
1°	8/64	0.9	0.7	0.8	2.3
	24/64	0.8	0.6	0.8	2.3
2°	8/64	1.6	1.0	0.8	1.6
	24/64	1.3	0.8	0.7	1.6
4°	8/64	3.8	2.5	1.5	0.7
	24/64	3.1	2.1	1.3	0.8

Despite the sizeable corruption in the reconstruction it still appears that correctly orientated projections are differentiated from reoriented projections (Table 3). To a large extent this ability to identify projections was independent of the degree of distortion (compare results for 8/64 versus 24/64 reoriented projections). Changing the orientation of the constructed projection, the correct reorientation can be identified for both rotation in the x axis (SSD/10³ figures highlighted in Table 4) and x translation (data not shown). The only exception was translation of 2 pixels (corresponding to the largest measured distortion) where the minimum SSD was identified at 1.5 pixels.

B. Investigating the limits of applicability

Results of the more detailed study are presented in Fig. 2 and Fig. 3. In Fig. 2, MSD between constructed and original projections is plotted versus angle (for combined right-angled pairs). The upper graphs show MSD for the object oriented correctly, whereas the lower graphs show MSD for the object rotated by 6 degrees. Noise mainly adds a bias to the MSD, maintaining the absolute difference between MSD for correctly aligned and mis-positioned projections. With

noise present, mis-positioned projections are more clearly identified when the object is reoriented. Application of a median filter reduced bias while maintaining identification of mis-positioned projections.

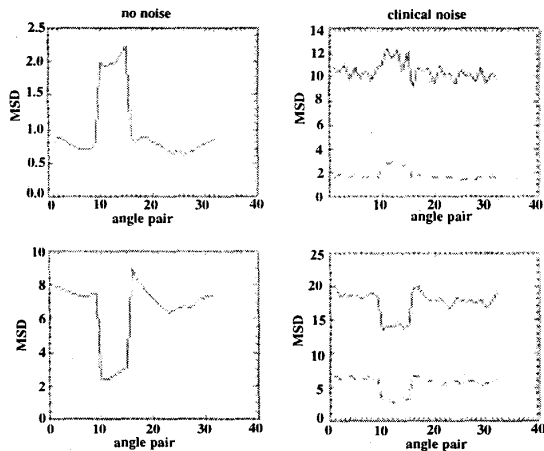


Fig. 2: Plots for MSD between constructed and original projections versus projection number. Angle pairs 10-16 are mis-positioned (3° x-axis rotation). Object is oriented correctly (above) and rotated 6° (below). Broken lines indicate median smoothing of projections.

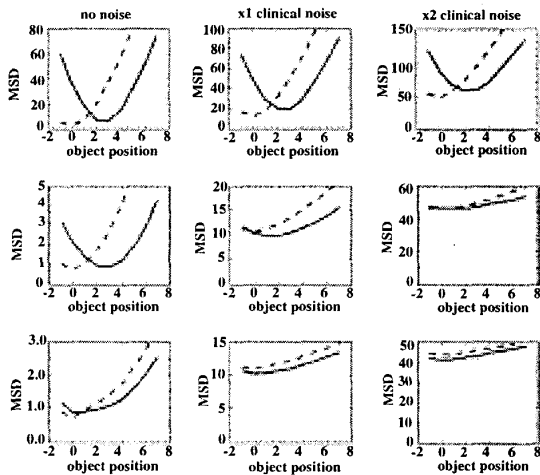


Fig. 3: Plots for MSD between constructed and original projections versus orientation of the reconstructed phantom. The top row is for 3 pixels x/y translation (z translation results are similar but not displayed). The middle row presents 3° x/y rotation, the bottom row 3° z rotation. In each case the dashed line represents the correctly aligned projections, the solid line represents the mis-positioned projections.

In Fig. 3, for each of the parameters, MSD is plotted versus orientation of the reconstructed object. The curves demonstrate the behaviour of the cost function for a correctly aligned projection and for a mis-positioned projection. It can be seen that translation in x/y provides clear discrimination between correctly aligned and mis-positioned projections, the minimum MSD being accurately defined, irrespective of the noise level. The addition of noise

increases the MSD as expected but does not appear to affect the overall discrimination between correctly aligned and mis-positioned projections. Even at extreme noise levels it should be possible to detect relatively small translations. In contrast the identification of rotation is less well defined and is more affected by noise, particularly for rotation around the z-axis. This probably is due to the symmetry of the phantom. There is relatively low distortion found on reconstructions based on projections with sizeable rotation (MSD for 2 degrees rotation ~ 0.2 MSD for 1 pixel translation), perhaps not surprising given that the influence on projections is relatively small.

C. Preliminary validation

Using the preliminary exploratory step, all mis-positioned projections were correctly identified with SSD increasing by typically 20 compared to aligned projections. Two slices of the reconstructed phantom are illustrated in Fig. 4 for motion-free, motion-corrupted and motion-corrected data. After correction with the proposed algorithm MSD was significantly reduced, with a reduction factor (RF), defined as $MSD_{\text{corrupt}} / MSD_{\text{corrected}}$, of 2.71 for the complete brain. For the displayed slices RF was 3.16 (upper slice) and 5.10 (lower slice). Reduction of motion artifacts is clearly evident in the subtracted images. Residual differences between motion-corrected and motion-free data may be further reduced with additional iterations.

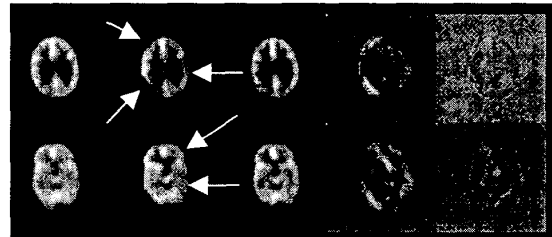


Fig. 4: Reconstructions for motion-free data (left), motion corrupted data (middle) and motion-corrected data (right). Motion-free minus motion-corrupted (mid-right); motion-free minus motion-corrected (far-right). Arrows indicate areas of apparent reduction in perfusion as a result of the motion.

IV. DISCUSSION

In this paper we present a new algorithm that permits data-driven correction for changes in patient position during emission tomography acquisition. The algorithm combines 3d registration with a method for sequentially updating the 3d reconstruction to include projection data at their correctly orientated position. The feasibility of the technique has been demonstrated and the algorithm was used to reduce the distortion due to a complex motion. These early findings are very promising, however, considerable additional work is necessary to fully explore the applicability of the technique.

Some insights to the applicability of the technique are presented. The ability to identify translated projections appears to be relatively insensitive to noise, presumably due

to the large differences found in projections compared to noise. This is not the case for rotation, especially around the z axis, where reorientation was hard to identify, even using the two orthogonal views. However, distortion in the reconstruction due to this rotation was also relatively small and therefore it may be less critical that this particular motion is exactly corrected. This will require verification for other movements and activity distributions.

There clearly are other factors that require further investigation. The corrupted initial reconstruction that incorporates wrongly positioned projections must be used to differentiate between correctly aligned and mis-positioned projections. However, it may be preferable to utilise only projections that are identified as correctly located as the initial estimate for reconstruction, building on this reconstruction as projections are reoriented. This needs more detailed analysis as it can be anticipated that there could be some lower limit in the number of projections (and iterations) that will provide accurate projections estimation.

The cost function used in this study was the mean square difference between constructed and original (measured) projections. Previous study of cost functions applicable to intra-subject SPECT registration demonstrated that this was preferable to alternative cost functions [13]. The simplex algorithm was used to find the 'best' orientation so as to minimize the cost function. This may not be optimal in terms of speed or susceptibility to local minima, however alternatives have not yet been explored.

The changes in patient position defined the grouping and ordering of projections rather than any considerations of maintaining subset balance that may be required by OSEM. Certainly for the dual head geometry assumed in this paper a subset size of 2 is suggested, smaller than normally recommended for OSEM. This may be cause for concern, although there appears to be no theoretical reason why the more exact rescaled block iterative (RBI) algorithm [14] could be used in place of OSEM. The RBI approach is not limited by subset imbalance such as may occur with two orthogonal views.

V. CONCLUSIONS

A hybrid 3d reconstruction / registration technique is presented that corrects for changes of patient position during emission tomography acquisition. There is considerable scope for additional work to identify the limits of applicability of the technique, likely to be influenced by the magnitude and timing of motion and the underlying activity distribution. However, these preliminary results demonstrate that the proposed technique shows considerable promise as an automated data-driven motion correction technique.

VI. REFERENCES

- [1] MV Green, J Seidel, SD Stein, TE Tedder, KM Kempner. "Head movement in normal subjects during simulated PET brain imaging with and without head restraint." *J. Nucl. Med.*, vol 35: pp1538-1546, 1994.
- [2] ME Daube-Witherspoon, YC Yan, MV Green, RE Carson, KM Kempner, P Herscovitch. "Correction for motion distortion in PET by dynamic monitoring of patient position." *J. Nucl. Med.*, vol 31: p816 (abs), 1990.
- [3] Y Picard, CJ Thompson. "Digitised video subject positioning and surveillance system for PET." *IEEE Trans. Med. Imag.*, vol 16: pp137-144, 1997.
- [4] BJ Lopresti, A Russo, WF Jones, T Fisher, DG Crouch, DA Altenburger, DW Townsend. "Implementation and performance of an optical motion tracking system for high resolution brain PET imaging." In EJ Hoffman (ed). *Proc. of 1998 IEEE Nucl. Sci. Symp. and Medical Imaging Conf.*, vol II, pp1127-1131, 1999.
- [5] RR Fulton, S Eberl, SR Meikle, BF Hutton, M Braun. "A practical 3D tomographic method for correcting patient head motion in clinical SPECT." *IEEE Trans. Nucl. Sci.*, vol 46: pp667-672, 1999.
- [6] M Menke, MS Atkins, KR Buckley. "Compensation methods for head motion detected during PET imaging." *IEEE Trans. Nucl. Sci.*, vol 43: pp310-317, 1996.
- [7] RR Fulton, BF Hutton, M Braun, B Ardekani, R Larkin. "Use of 3D reconstruction to correct for patient motion in SPECT." *Phys. Med. Biol.*, vol 39: pp563-574, 1994.
- [8] J Li, RJ Jaszczak, RE Coleman. "A filtered backprojection algorithm for axial head motion correction in fan-beam SPECT." *Phys. Med. Biol.*, vol 40: pp2053-2063, 1995.
- [9] LK Arata, PH Pretorius, MA King. "Correction of organ motion in SPECT using reprojection data." In *Proc 1995 IEEE Nucl. Sci. Symp. and Medical Imaging Conf.*, pp 1456-1460, 1995.
- [10] KJ Lee, DC Barber. "Use of forward projection to correct for patient motion during SPECT imaging." *Phys. Med. Biol.*, vol 43: pp171-187, 1998.
- [11] AJ Britten, F Jamali, JN Gane, AEA Joseph. "Motion detection and correction using multi-rotation 180° single-photon emission tomography for thallium myocardial imaging". *Eur. J. Nucl. Med.*, vol 25: pp 1524-1530, 1998.
- [12] HM Hudson, RS Larkin. "Accelerated image reconstruction using ordered subsets of projection data." *IEEE Trans. Med. Imag.*, vol 13: pp601-609, 1994.
- [13] S Eberl, I Kanno, RR Fulton, A Ryan, BF Hutton, MJ Fulham. "Automated interstudy image registration technique for SPECT and PET." *J. Nucl. Med.*, vol 37: pp137-145, 1996.
- [14] C L Byrne. "Accelerating the EMLL algorithm and related iterative algorithms by rescaled block-iterative (RBI) methods." *IEEE Trans. Image Processing*, vol 7: pp100-109, 1998.